Cirrus Cloud Properties Derived from the First Year of Millimeter Wave Cloud Radar Data

G. G. Mace
Department of Meteorology
University of Utah
Salt Lake City, Utah

E. E. Clothiaux
Department of Meteorology
The Pennsylvania State University
University Park, Pennsylvania

Introduction

The representation of cirrus clouds in large-scale models continues to be a problem of considerable contemporary importance. These cloud systems occur over vast areas of the earth's surface, tend to occur in all climatic regimes and demonstrate a high degree of variability in their macro and microphysical properties (Liou 1986). Furthermore, cirrus can significantly influence the overall heating of the atmosphere and surface (Stephens et al. 1990); the sign of the heating can be positive or negative and depends primarily on the cloud properties.

While several field programs in the last decade have provided a clearer understanding of cirrus clouds, the short duration of these programs preclude all but the broadest generalizations on typical cirrus properties or the relationship of these properties to the atmosphere in which they evolve. In other words, while we are able to place important cirrus properties into a particular parameter range, we are not, as yet, able to assign values to terms such as mean and standard deviation of particular cloud properties in a given dynamical setting. Defining the means and standard deviations for the important cloud properties as well as coming to some understanding as to what drives these distributions will be key in improving the representation of clouds in climate models.

The above reasoning served as the primary motivation for a study of cirrus macroscale properties by Mace et al. (1997; hereafter referred to as M97). M97 used approximately 900 hours of cloud radar data collected during a 2½-month period over central Pennsylvania to investigate such properties as cirrus base, top, layer thickness, and the vertical distribution of radar reflectivity within cirrus layers. By combining the radar data with output from a mesoscale model, the relationships between certain cloud properties and the large-scale temperature and vertical velocity were also considered. In the present paper, we examine cirrus cloud properties following the general approach of M97 and use a one-year record of 35 GHz radar data (as well as other data) collected at the Atmospheric Radiation Measurement (ARM; Stokes and Schwartz 1994) site in north-central Oklahoma. Since the record is longer and a larger suite of instrumentation is available, we examine the interseasonal variation of macroscale cirrus properties as well as the bulk microphysical properties and their relationships to temperature and large-scale ascent.

Results: Macroscale Properties

We examine approximately 12,500 hours of radar data collected between November 1996 and February 1997. Cirrus are defined as a layer of significant radar echoes separated from lower layers that has the reflectivity maximum at a temperature colder than -40^o C. Figure 1 presents monthly means of several fundamental statistics. The occurrence frequency of cirrus (defined as that fraction of profiles that have at least one cirrus layer) shows well-defined seasonal oscillations and ranges from a minimum of 10% in November 1997 to a maximum near 30% in May 1997. Winter 1996/1997 had a nearly constant frequency near 27%. The fraction drops during the early spring of 1997 and rises as the convective season in Oklahoma begins in May. A significant decrease in occurrence is noted after July 1997. This decrease continues until November 1997 when the occurrence increases somewhat during the winter of 1997/1998. A large difference in cirrus occurrence between the two winters is evident, however, additional data collection is needed to determine if this difference is related to the strong 1997 El-Niño Southern Oscillation (ENSO).

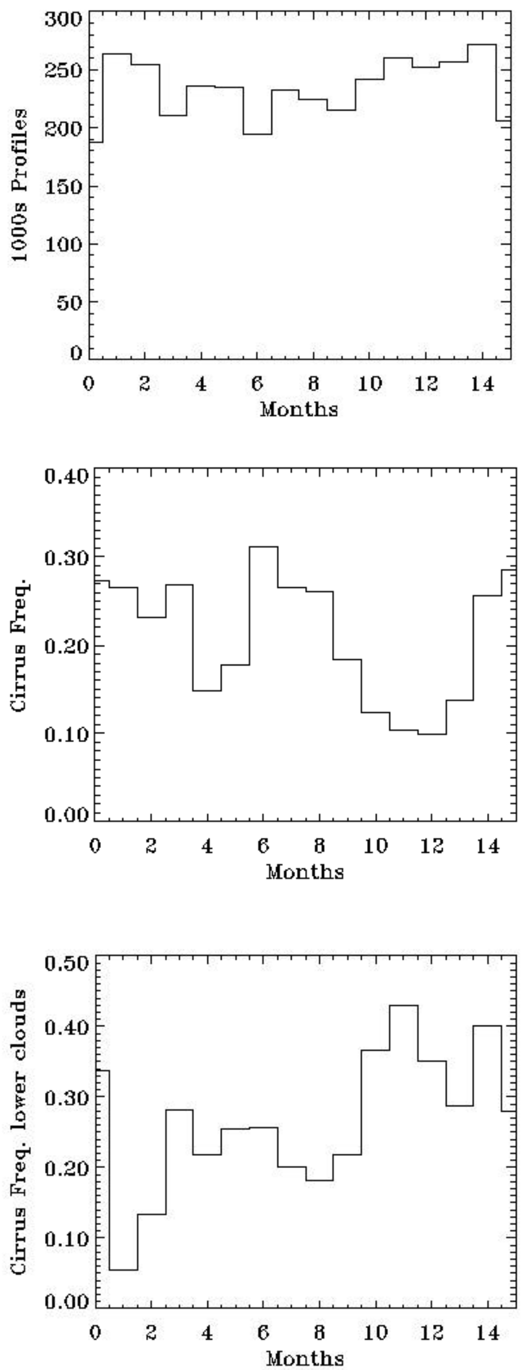

Figure 1. Monthly mean statistics for the period starting in November 1996 and extending through February 1998. a) The number of radar profiles examined each month. b) The fraction of profiles with at least one cirrus layer. c) The fraction of cirrus profiles that occurred with lower clouds present.

The fraction of time lower layers occur with cirrus is shown in Figure 1b. This statistic is much more sporadic with a mean near 22% of the time and a range between 5% and 42%. It is interesting to note that the season with the highest lower cloud statistic (autumn 1997) is also the period with the lowest overall frequency of cirrus occurrence. A significant difference between the winters is also evident in this statistic with lower clouds occurring much less during the 1996/1997 winter season. Again, this may be related to anomalous cloudiness related to perturbed synoptic-scale patterns during the ENSO year of 1997/1998.

Figure 2 shows annual means of several macroscale properties related to the vertical distribution of cirrus clouds. Because cloud base and top are critical to the overall net heating rate through the upwelling and downwelling thermal radiation, their correct representation in climate models are important. We find cirrus clouds, as defined here, tend to have bases most commonly near 9 km and tops near 10.5 km. Both of these statistics have rather large variances, however. The layer tops distribution is limited above by the statistical location of the tropopause as can be seen in Figure 2d. We find the tops of cirrus occur most often within 1 km of the tropopause with a few instances of layer tops up to 1.5 km above the tropopause. These cases of cirrus tops extending above the tropopause occurred during the months of May and June 1997 during the peak of the spring convection season in the central United States. The layer thickness distribution peaks near 1 km. This is an important result because most GCMs do not parameterize the vertical subgridscale depth of clouds, and 1 km is generally only about half of the typical vertical resolution of most GCMs.

Comparison of these results with M97 shows many similarities. In general, the cirrus observed in Oklahoma occurred slightly higher in the atmosphere, at colder temperatures and had somewhat higher radar reflectivities. The increased sensitivity of the ARM radar may be at least partially responsible for these differences. The cirrus examined by M97 occurred most frequently approximately 1 km below the tropopause at temperatures near -40° C; while, in the ARM dataset, cirrus occurred most often near -45° C. The most likely radar reflectivity of the cirrus in the M97 data set was near -24 DbZe; while, in the present study, the most likely radar reflectivity is near -20 DbZe. Both data sets show a weak positive correlation of temperature with reflectivity. The correlation is slightly more positive in the ARM data than in the data collected at Penn State. The manner in which the radar reflectivity in a cirrus layer is distributed vertically tends to be a strong function of layer depth in both data sets; as a layer becomes thicker, the total

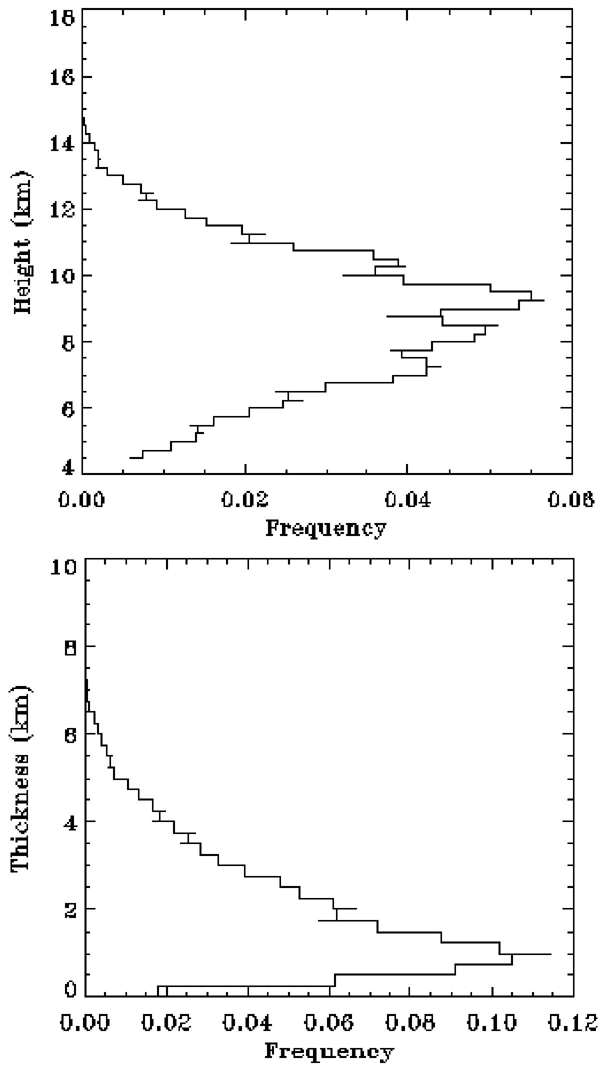

Figure 2. Period-averaged (November 1996 to February 1998) vertical distributions of a) cloud base, b) cloud top, c) layer thickness and d) distance of cloud top from the tropopause.

layer reflectivity tends to become concentrated in the middle one-third of the layer. Presumably, cirrus ice crystals tend to grow as they fall through ice saturated layers from the nucleation zone near cloud top. Based on this interpretation, the lower one-third of the layer is dominated by sublimating ice crystals.

Results: Bulk Microphysical Properties

A major advantage of the present data record over that used by M97 is the availability of data from additional instrumentation. This allows us to examine bulk micro-physical properties retrieved by combining the radar data with other observations. We use results from the radiance-reflectivity algorithm described by Mace et al. (1998). This algorithm combines the radar reflectivity with infrared radiances observed by the atmospheric emitted radiance interferometer (AERI). The radiance-reflectivity algorithm is limited by the AERI temporal resolution (3-minute dwell every 8 minutes) and requires optically thin cirrus with no lower clouds. The algorithm estimates the first-order modified gamma distribution averaged through the layer that generates the observed radar reflectivity and, when the cloud properties are inserted into a radiation transfer model, generates the observed downwelling radiance. The con-straints on the algorithm limit any broad interpretation on the general properties of cirrus. However, since we have applied the algorithm to all possible cases during the period under study, the properties of the optically thin cirrus layers that occurred over the ARM site during this 15-month period can be examined in unprecedented detail.

Figure 3 shows the frequency distributions of layer-mean ice water content (IWC), effective radius (r_e), and total particle concentration (*N*). We divide the distributions into two populations segregated by layer-mean temperature. We term cold cirrus as the coldest one-third of the distribution and warm cirrus as the warmest one-third. The temperature cutoffs are approximately 221 K and 227 K, respectively. For the IWC (Figures 3a and b) we find that the most likely IWCs are the smallest regardless of temperature with an approximate exponential decrease in frequency for larger IWC values. Several large-scale cirrus parameterizations used in GCMs assume that the IWC is directly proportional to temperature. We do find a temperature dependence that acts to broaden the warm cirrus IWC distribution and moves the mean IWC toward higher values. However, the overall shape of the warm cirrus distribution is similar to the cold and the most probable IWC is still the smallest.

The effective radius, r_e, (defined as the ratio of the third to the second moment of the particle size distribution) and the total particle concentration, *N*, both show a more significant dependence on temperature compared to the IWC. The modal value of r_e shifts from near 25 μm for the cold cirrus to near 50 μm with a much broader distribution for the warm cirrus. Conversely, colder cirrus appear much more likely to have higher values of *N* than their warm counterparts. This oppositely trending behavior with temperature for r_e and *N* explain the relatively weaker temperature dependence seen in the IWC with warmer cirrus more likely to have low concentrations of large particles and cold cirrus to have high concentrations of small particles. These results also have obvious implications for the impact of cirrus on the radiation streams. For a given water path, cirrus that exist at colder temperatures will have a comparatively larger optical depth due to the smaller particles than warmer cirrus and, thus, will impact the solar and infrared radiation to a greater degree.

Summary and Conclusions

We have examined the statistical distributions of cirrus cloud properties derived from 15 months of cloud radar and other data collected at the ARM site in Oklahoma. We find that the cirrus observed at the ARM site are very similar in their macroscale properties to the cirrus examined by M97. The slight differences seen between the two data sets are likely due to the increased sensitivity of the ARM cloud radar compared to the Penn State radar system used by M97. We have also examined distributions of bulk microphysical properties of the cirrus during the 15-month period that were optically thin and occurred with no lower clouds present. We find that the effective radius and total particle concentration have a significant, though opposite, temperature dependence. This finding helps us understand the relatively weaker dependence of IWC on temperature.

The case study mentality driven by the short duration of past field programs have precluded any quantitative validation of cirrus properties parameterized by large scale models. Since large-scale models predict cloud properties averaged over long time steps and large areas, the snapshots provided by occasional aircraft penetrations make intercomparison quite difficult. Not only is the accuracy of the large scale dynamics difficult to evaluate in individual case studies, but the influence of factors, such as the horizontal advection of ice into the area under consideration, is nearly impossible to ascertain at the present time. The results presented in the present study should represent the beginning of a paradigm shift in the validation of cloud parameterizations. We are now able to examine bulk statistics of cirrus clouds using output from algorithms applied to remote sensing data. Instead of using infrequent aircraft observations as a primary tool for validation, we can use the observed in situ microphysics to validate the remote sensing algorithms. Results from the validated algorithms can then be applied to extended periods to validate the model parameterizations using statistical distributions of macro- and microphysical properties. This approach will allow us to more thoroughly examine the validity of the cloud properties predicted by large-scale models. Assuming that the climate of the model is similar to the actual climate, we would expect that over a long time period, the model would generate cloud property distributions similar to that observed in the atmosphere.

Our present and future work is moving in the direction outlined by the previous paragraph. We will continue to extend the length of the data set under consideration as long as ARM continues to collect cloud radar data. We have also initiated collaboration with leading research groups developing and running global climate models. Initial studies comparing annually and seasonally-averaged cirrus cloud properties are ongoing. The algorithms currently being used to retrieve the microphysics properties of clouds from the remotely sensed data are limiting in the sense that only a subset of clouds can be examined. We are, therefore, developing a new generation of cirrus algorithms that use the Doppler moments instead of just the radar reflectivity and radiometer observations. Similar efforts are under way to develop more general algorithms for evaluating the properties of liquid phase clouds. These algorithms will be validated by the wealth of in situ data that is now available from several intensive observation periods conducted at the ARM site.

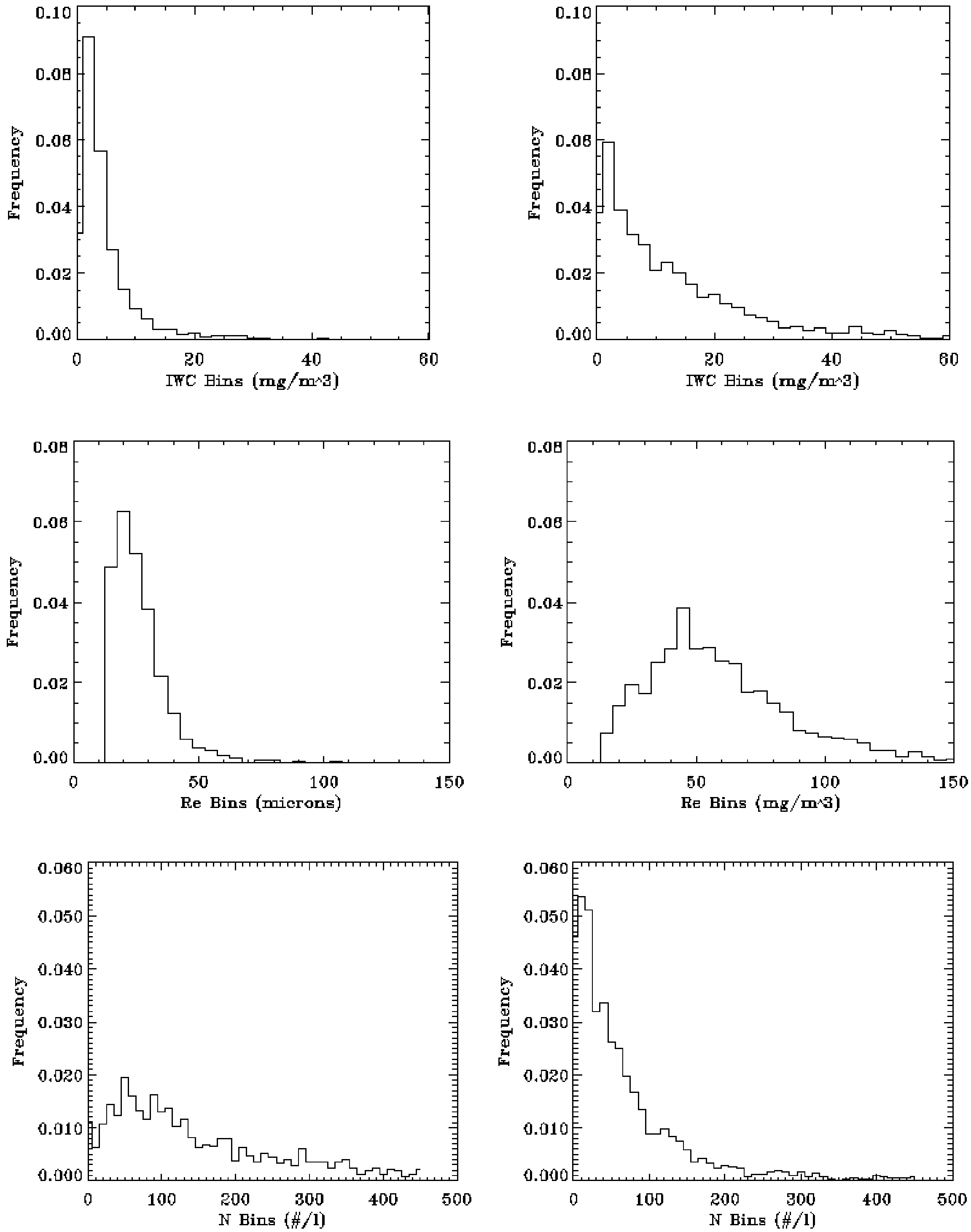

Figure 3. Frequency distributions retrieved from combined radar and AERI data of a) IWC, b) r_e, and c) total particle concentration averaged over all optically thin cirrus layers that occurred with no lower clouds present.

References

Liou, K. N., 1986: Influence of cirrus clouds on weather and climate: A global perspective. *Mon. Wea. Rev.,* **114,** 1167-1199.

Mace, G. G., T. P. Ackerman, E. E. Clothiaux, and B. A. Albrecht, 1997: A study of composite cirrus morphology using data from a 94-GHz radar and correlations with temperature and large-scale vertical motion. *J. Geophys. Res.*, **102,** 13,581-13,593.

Mace, G. G., K. Sassen, S. Kinne, and T. P. Ackerman, 1998: An examination of cirrus cloud characteristics using data from millimeter wave radar and lidar: The 24 April SUCCESS case study. *Geophys. Res. Lett.*, **25,** 1133-1136.

Stephens, G. L., S. Tsay, P. W. Stackhouse, Jr., and P. J. Flatau, 1990: The relevance of the microphysical and radiative properties of cirrus clouds to climate and climatic feedback. *J. Atmos. Sci.*, **47,** 1742-1753.

Stokes, G. M., and S. E. Schwartz, 1994: The Atmospheric Radiation Measurement (ARM) Program: Programmatic background and design of the cloud and radiation test bed. *Bull. Amer. Meteor. Soc.*, **75,** 1201-1221.